



Cite this: *Chem. Sci.*, 2025, **16**, 18496

All publication charges for this article have been paid for by the Royal Society of Chemistry

Received 11th September 2025
Accepted 24th September 2025

DOI: 10.1039/d5sc07001e
rsc.li/chemical-science

Chiral heterogeneous photocatalysts for enantioselective synthesis: standing on the shoulders of organocatalysis

Camilla Callegari, ^a Marco Moroni, ^b Davide Ravelli ^{*a} and Lorenzo Malavasi ^{*b}

Crafting organic molecules with control over their absolute stereochemistry is a challenging task for synthetic chemists. The present Perspective encompasses recent examples of enantioselective transformations based on chiral heterogeneous photocatalysts, including metal–organic frameworks (MOFs), covalent organic frameworks (COFs) and hybrid metal–halide perovskites (MHPs). Such materials combine a photocatalytic unit and a chiral element in a single component: the former is responsible for substrate activation, while the latter, typically a small organic molecule – *i.e.*, an organocatalyst –, takes care of stereoinduction instead. Although synthetic applications are still limited to a handful of (benchmark) C–C and C–N bond formations and oxidation protocols, their number is expected to grow steadily in the near future. This trend is supported by cross-disciplinary knowledge transfer from the field of asymmetric organocatalysis, which is also driving the application of these materials in broader areas, such as solar-to-chemical energy conversion and chiral sensing technologies.

Introduction

Chirality is a fundamental geometric property, which applies when a generic object cannot be superimposed onto its mirror image, just like it happens for human hands. In chemistry, the two mirror images of a chiral molecule are named enantiomers and their different behavior in a chiral context is at the basis of a wide range of disciplines, notably in biological settings and technological applications.¹ Thus, it comes as no surprise that chiral molecules are ubiquitous among pharmaceuticals and agrochemicals,^{2,3} and they also represent a significant share in the field of materials science.⁴

In recent years, asymmetric catalysis, namely the exploitation of a chiral catalyst to orchestrate and direct the stereochemical course of synthetic transformations, has emerged as a powerful strategy to promote the preferential formation of one specific stereoisomer, including the preparation of enantioselectively pure compounds.^{5–7} Among the available approaches, the 2021 Nobel-prize winning methodology of “asymmetric organocatalysis” undoubtedly represents a cornerstone in the field.⁸ Starting from the late 90s, this strategy, which employs catalytic amounts of small chiral organic molecules to convert the substrate(s) of interest, has experienced an impressive development, becoming one of the major pillars of asymmetric

catalysis.^{9–12} This success is mostly based on its operational simplicity (ambient conditions, aqueous solvents, *etc.*) and metal-free nature, which well align with the general requirements of Green Chemistry.¹³ Frequently, these organocatalysts feature nitrogen-containing functionalities, notably amines, conveniently derived from naturally occurring compounds, including alkaloids and amino acids (*e.g.*, proline or phenylalanine).^{14–21} As an alternative, widely appreciated organocatalysts pertain to the families of (thio)urea^{22–25} and BINOL²⁶ (1,1'-bi-2-naphthol) derivatives.

In parallel, visible-light photocatalysis has entered the scene of organic chemistry, offering synthesis practitioners with a myriad of opportunities to design radical-mediated transformations.²⁷ In such manifold, traceless photons are absorbed by a competent catalyst (tagged “photocatalyst” – PC –), being either a molecular species soluble in the reaction medium (homogeneous photocatalysis) or a solid semiconducting material (heterogeneous photocatalysis).²⁸ Independently from its physical state, the photocatalyst is in turn responsible for substrate activation when in the excited state. This leads to the generation of highly reactive open-shell intermediates under controlled conditions, increasing reaction efficiency, also thanks to the noteworthy functional group tolerance integral to radical species.²⁹ Intriguingly, photocatalytic transformations can be realized in an asymmetric fashion as well, by integrating a component able to control the stereochemical course of the process into the photocatalytic system.^{30–32} Despite the inherent practical advantages, including easier catalyst separation and recyclability, facilitated product isolation, and improved cost-

^aPhotoGreen Lab, Department of Chemistry, University of Pavia, 27100 Pavia, Italy.
E-mail: [davide.ravelli@unipv.it](mailto: davide.ravelli@unipv.it)

^bEnergy and Materials Chemistry Group, Department of Chemistry and INSTM, University of Pavia, 27100 Pavia, Italy. E-mail: [lorenzo.malavasi@unipv.it](mailto: lorenzo.malavasi@unipv.it)



effectiveness, the field of asymmetric heterogeneous photocatalysis is still in its infancy.^{33–36} Nevertheless, it is expected to grow steadily in the near future, due to the impressive progress related to the design and engineering of materials.³⁷

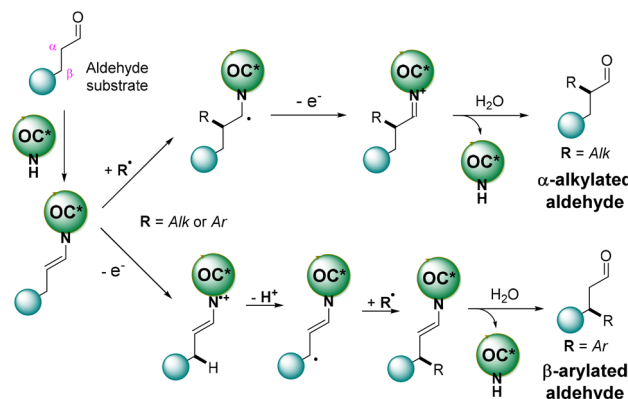
State-of-the-art strategies in this area essentially involve translating knowledge from homogeneous photocatalysis (Scheme 1a) to its heterogeneous variant. Along this line, a convenient approach takes inspiration from dual-catalytic methodologies based on the synergy between asymmetric organocatalysis and photocatalysis, wherein substituting the original (homogeneous) photocatalyst with a heterogeneous one characterized by analogous redox properties has been demonstrated as a robust choice³⁸ (Scheme 1b). Recently, however, several research groups have been active in the preparation and application of chiral materials, embedding both the photocatalytic component and a unit responsible for stereocontrol in a single entity. As a matter of fact, only a handful of different materials have been adopted in the role of chiral heterogeneous photocatalysts (Scheme 1c). In virtue of their wide tunability and design potential, most examples are based on Metal–Organic Frameworks (MOFs)³⁹ and Covalent Organic Frameworks (COFs),^{40,41} involving a chiral component (e.g., an amine or a BINOL derivative), which is integral to their crystalline structures. To have insights into the indicated classes of materials, the reader is invited to peruse the excellent reviews recently appeared in the literature. At the same time, an emerging area involves the use of metal halide perovskites^{42,43} in the form of nanocrystals (MHP-NCs) as heterogeneous photocatalysts, whose surface has been covered with a layer of a chiral amine.

As apparent, the very same compounds typically exploited in the realm of asymmetric organocatalysis can be conveniently harnessed for the preparation of chiral heterogeneous photocatalysts, which are the main focus of the present Perspective along with the inherent asymmetric synthetic applications. In the following, the mode of action of the different materials is detailed with respect to the photoactive and the organocatalytic unit, respectively, while synthetic transformations have been listed according to the developed application. At the same time, this work does not address neither examples involving photoactive supramolecular cages, nor reports on direct

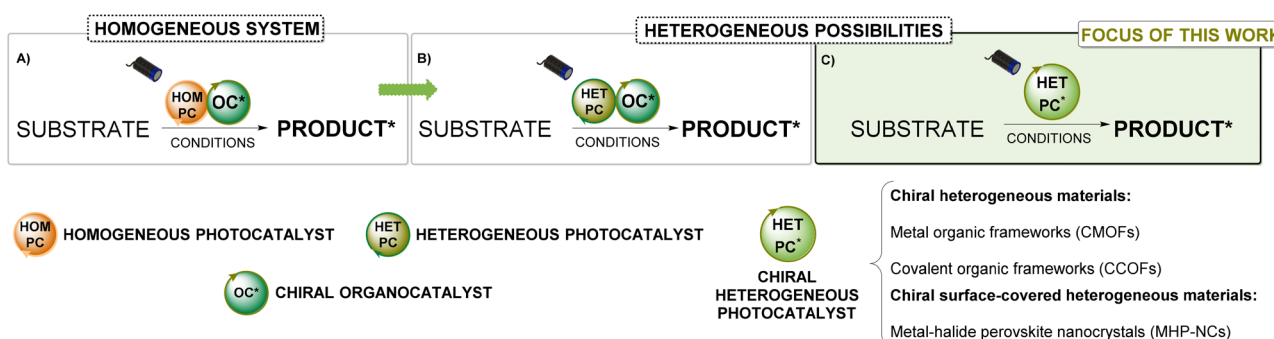
photochemical transformations occurring within confined supramolecular cavities.⁴⁴

Application of chiral heterogeneous photocatalysts in asymmetric synthesis

The number of examples exploiting chiral heterogeneous photocatalysts in asymmetric synthesis is still limited. A significant fraction of reports deals with a benchmark reaction in the field of asymmetric photocatalysis performed under homogeneous conditions, namely the α -alkylation of aldehydes.⁴⁵ Accordingly, it is possible to compare the performance of different materials toward the same transformation and discuss pros and cons of the available methodologies.^{46–48} At the same time, by modifying the electrons flow within the photocatalytic system, it has been possible to divert the asymmetric functionalization (specifically, arylation) of aldehydes to the β -position,⁴⁹ again mimicking a transformation known in the homogeneous field.⁵⁰ In these examples, the organocatalytic component of the reaction system (a secondary amine derivative) undergoes condensation with the aldehyde substrate to deliver an enamine. Thanks to the stereochemical information embedded in the organocatalyst, it is then possible to discriminate between the two faces of the enamine intermediate, delivering the final enantioenriched product (Scheme 2).



Scheme 2 Mechanistic scenario operating in the asymmetric α -alkylation and β -arylation of aldehydes via a common enamine intermediate.



Scheme 1 Asymmetric photocatalytic syntheses under: (a) homogeneous or (b) heterogeneous conditions. (c) Known examples of chiral heterogeneous photocatalysts treated in this Perspective.

Apart from C–C bond formation, the described reactivities have been extended to the selective oxidation of sulfides to chiral sulfoxides as well.⁵¹ Finally, one of the most recent examples deals with the synthesis of axially chiral N-heterocycles *via* C–N bond formation.⁵²

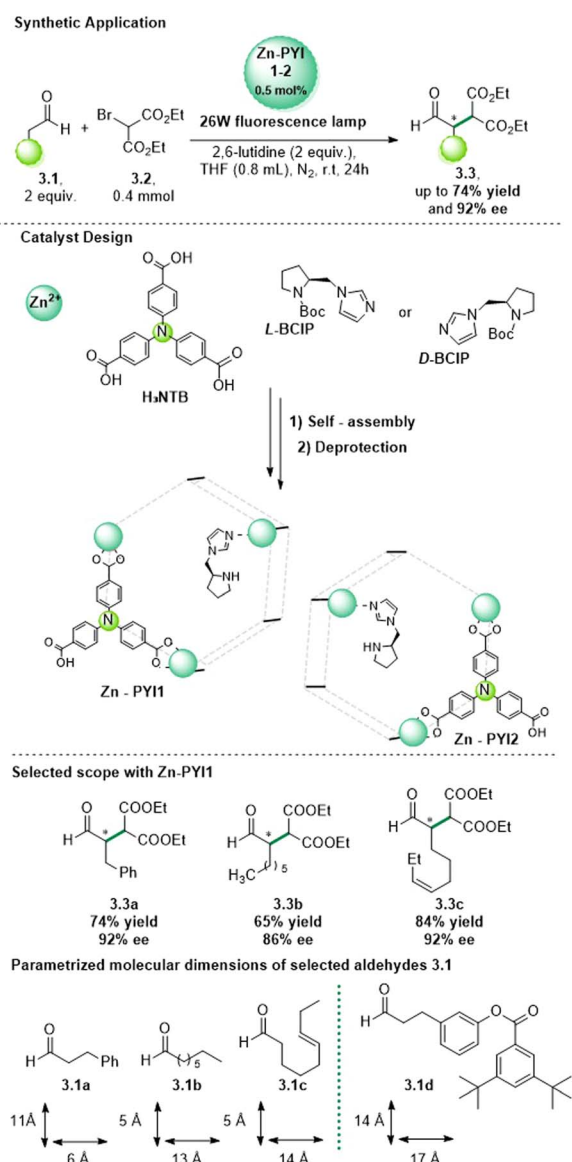
C–C bond formation

A seminal contribution in the field of C–C bond formation deals with a 2012 report from Duan's group, who incorporated a chiral organocatalyst into a photoactive Metal–Organic Framework (MOF).⁴⁶ Such design unlocked the preparation of a synergistic catalyst integrating both photocatalytic and organocatalytic units (Scheme 3).

Specifically, they synthesized a chiral metal–organic framework (CMOF)⁵³ by assembling the chiral organocatalyst *L*- or *D*-

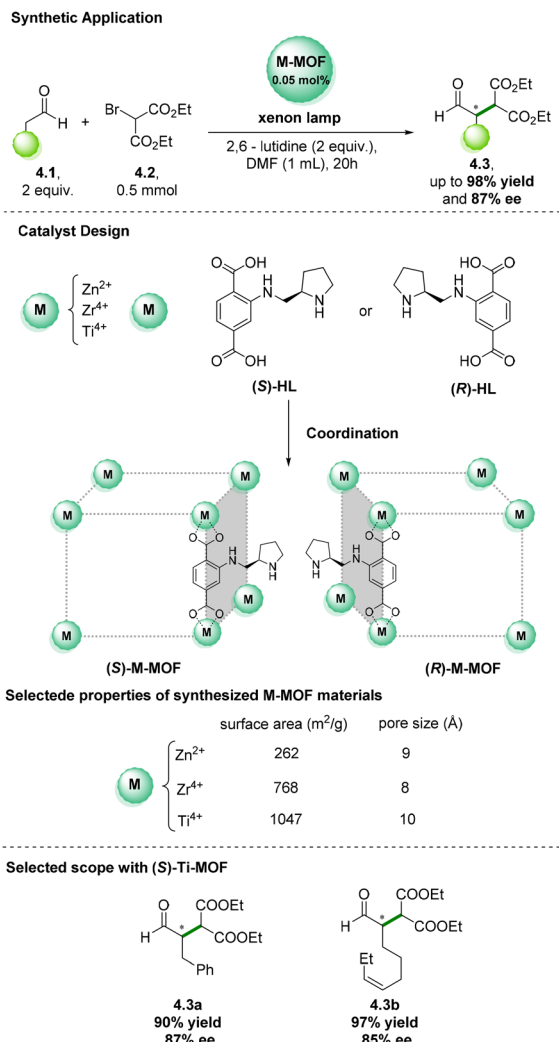
pyrrolidin-2-ylimidazole (**PYI**) with a triphenylamine-based photoredox scaffold (*4,4',4''*-nitrilotrisbenzoic acid, **H₃NTB**) and the Zn²⁺ cation into a single framework. Briefly, a Boc-protected derivative of the organocatalyst, namely *N*-*tert*-butoxycarbonyl-2-(imidazole)-1-pyrrolidine (**BCIP**) was adopted in a self-assembly process along with the other components. The resulting structure features a two-dimensional, brick wall like layered framework, showing a regular packing pattern that gives rise to 1D channels with dimensions of 12 × 16 Å². Upon deprotection, this strategy produced two enantiomeric heterogeneous photocatalysts, **Zn-PYI1** and **Zn-PYI2**, from *L*- and *D*-**BCIP**, respectively. Both materials are characterized by an organocatalytic active site, *viz.* the secondary N–H amine of pyrrolidine, exposed within their channels. As depicted in Scheme 3, these photocatalysts were subsequently tested in the asymmetric light-driven α -alkylation of aliphatic aldehydes **3.1** with α -halogenated carbonyls **3.2**, delivering the expected products **3.3** in good yields (up to 74%) and enantiomeric excesses as high as 92%. Interestingly, a good reactivity profile was observed when the molecular size of the aliphatic aldehydes **3.1** matched the pore dimensions of the catalyst, allowing the substrates to pass through its channels (see the case of **3.1a–c**); on the other hand, **3.1d** did not fit into the pores and showed a poor conversion (<10%), accordingly. Such size-selectivity suggests that the alkylation reaction primarily occurs within the catalyst's channels, wherein the formation of the requisite enamine intermediate from the reaction between the aldehyde substrate and the chiral component incorporated into the catalyst (see Scheme 2 above) can take place, rather than on its external surface. Notably, the enantioselectivity was maintained over three cycles of catalyst reuse.⁴⁶

Another example of visible-light-driven heterogeneous catalytic system for the asymmetric α -alkylation of aldehydes has been reported by Tang and colleagues.⁴⁷ In their approach, different chiral metal–organic frameworks (CMOFs) were designed by assembling the same chiral organic molecule with various metal ions, such as Zn²⁺, Zr⁴⁺ and Ti⁴⁺. Remarkably, the prepared frameworks (labelled **M-MOF**, with M = metal ion) demonstrated significant catalytic performance under visible light irradiation, in a process that could be finely tuned by simply varying the metal ion, thanks to the tunable electron transfer dynamics between the chiral ligand and the metal centers (Scheme 4). In particular, the organic component acting as the MOF linker (tagged *(R)*–*(S)*–**HL**) was prepared by reacting protected *N*-(*tert*-butoxycarbonyl)-prolinal (*N*-Boc-prolinal), a proline derivative, with 2-aminoterephthalic acid (**H₂BDC-NH₂**) in a Schiff base condensation/reduction sequence. The terephthalic acid derivative has been selected for two key reasons: its carboxylic acid groups readily coordinate with metal ions for MOF assembly, and its aromatic group may enhance photocatalytic performance by facilitating photoinduced charge separation. Together, these components served as the building blocks of the CMOF which, after Boc-protecting group removal, was then applied to asymmetric C–C bond formation between aldehydes **4.1** and diethyl bromomalonate **4.2**. From a synthetic point of view, the as prepared (chiral) organic component *(S)*- or *(R)*–**HL** showed a modest reactivity only upon irradiation with



Scheme 3 Chiral metal–organic frameworks (CMOFs) for the light-driven asymmetric α -alkylation of aldehydes.



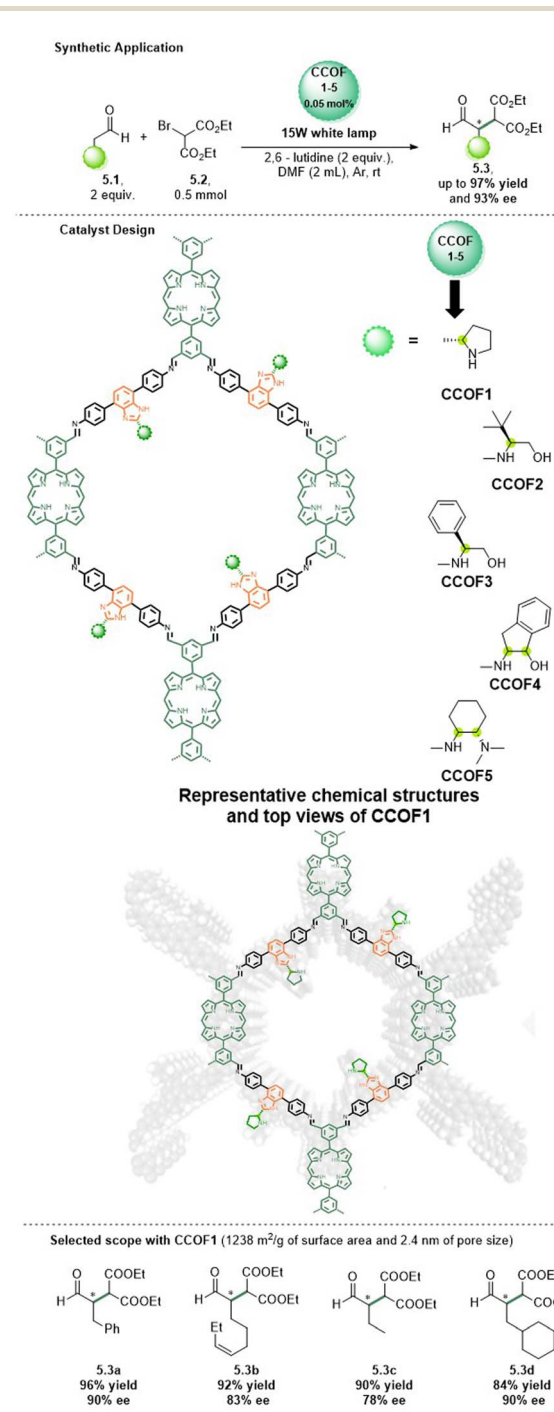


Scheme 4 Tunable chiral metal–organic frameworks (CMOFs) for the light-driven asymmetric α -alkylation of aldehydes.

high-power visible light (200 W), achieving moderate conversion (50–55%) and enantiomeric excess (up to 78%) in the α -alkylation of model aldehyde 3-phenylpropionaldehyde **4.1a** to deliver product **4.3a**. However, a significant reactivity enhancement was observed upon formation of the MOF material through coordination with the appropriate metal cation. In such case, the best performance was offered by the Ti-based material, characterized by the highest surface area ($1047 \text{ m}^2 \text{ g}^{-1}$) and pore size (around 10 \AA) among all the M-MOFs tested. Thus, upon irradiation with a low intensity light source (25 W), a long-lived ligand-to-metal charge transfer state was formed, resulting in up to 98% yield and up to 87% ee for products **4.3**. Moreover, the same CMOF heterogeneous photocatalyst demonstrated excellent stability and reusability, maintaining its crystalline structure and catalytic performance for three consecutive photocatalytic cycles.

Apart from CMOFs, chiral covalent organic frameworks (CCOFs)^{40,41} have been successfully employed as visible-light-driven heterogeneous chiral catalysts for the α -alkylation of aldehydes **5.1**. Thus, the group of Zhao developed a general

bottom-up strategy for constructing a series of photoactive CCOFs (Scheme 5).⁴⁸ The design incorporates porphyrin-based photoactive building blocks and chiral secondary amine-based catalytic centers, that are introduced into the framework by immobilization on the pore walls through benzimidazole linkers. In terms of catalytic activity, the former components function as light-harvesting units, generating photo-induced



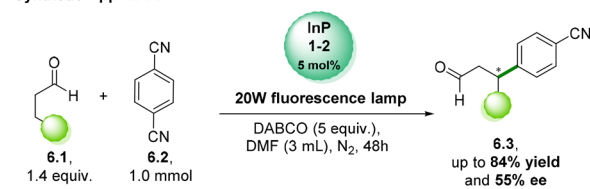
Scheme 5 Photoactive chiral covalent-organic frameworks (CCOFs) for the light-driven asymmetric α -alkylation of aldehydes. Adapted with permission from ref. 48. Copyright © 2023, American Chemical Society.

charge carriers essential for the activation of α -bromo carbonyls, while the latter conveniently interact with the aldehydes for stereocontrol. This dual-function system enabled efficient substrate activation and asymmetric induction within a confined, crystalline environment. The resulting CCOFs exhibited excellent catalytic performance, delivering the desired α -alkylated aldehyde products **5.3** in up to 97% yield and enantiomeric excess (ee) of up to 93%.

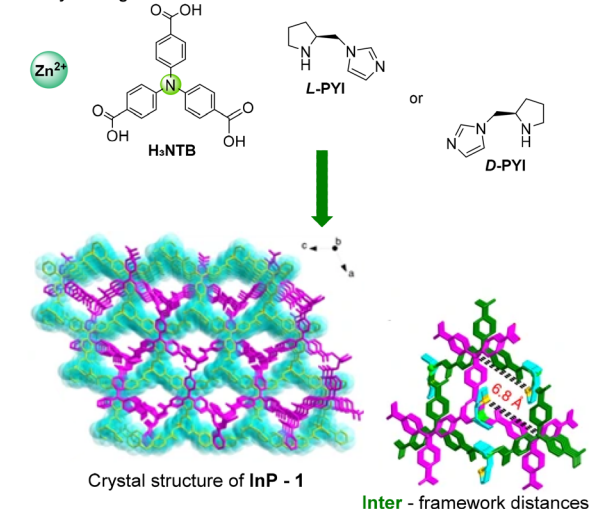
A specific application of CCOFs involves the asymmetric α -benzylolation of aldehydes under photothermal conditions,⁵⁴ wherein the energy input by photons is converted into thermal energy to trigger the transformation of interest.⁵⁵ Along this line, the Dong group designed and prepared a chiral COF catalyst by integrating chiral BINOL-phosphoric acid units and Cu(II)-porphyrin modules as photosensitizers *via* imine condensation, resulting in the formation of (*R*)-CuTAPBP-COF. This catalyst features synergistic Brønsted and Lewis acidic sites, a robust chiral confinement environment, and can trigger efficient visible-light-driven conversion. A broad range of aldehydes and benzyl halides were successfully transformed using this system, delivering excellent yields (91–98%) and enantioselectivities (91–94% ee), with the exception of substrates bearing bulky substituents. Although the mechanism has not been fully clarified yet, it has been demonstrated to involve radical intermediates *via* photothermal conversion.⁵⁴

Building on the work⁴⁶ described in Scheme 3 demonstrating that the integration of a photocatalyst and a chiral organocatalyst into a single MOF is an effective strategy for the α -functionalization of saturated carbonyls, the Duan group discovered that modification of the electron transfer pathways in heterogeneous photochemical transformations can be used to control the regioselectivity of the functionalization.⁴⁹ Specifically, they prepared an interpenetrated chiral MOF (CMOF) catalyst (**InP-1**) *via* a solvothermal reaction involving *L*-pyrrolidin-2-ylimidazole (*L*-PYI), 4,4',4''-nitrilotrisbenzoic acid (**H₃NTB**), and Zn(NO₃)₂·6H₂O, whose chirality was confirmed by circular dichroism (CD), with a positive Cotton effect. Thus, by tuning the electron transfer between the two active sites within the MOF, they introduced a strategy for achieving β -functionalization of saturated ketones and aldehydes **6.1** (Scheme 6).⁴⁹ This approach is feasible because the reduced interframework distances in **InP-1** accelerate electron transfer between the catalytic sites, promoting the formation of β -enaminy radicals. When this catalyst was employed on valeraldehyde and other more complex aldehydes, conversions between 69 and 84% were achieved, with enantiomeric excesses as high as 55%. The pore size of the catalyst (around 7 Å) was also critical to the success of the reaction, in analogy to the reactivity cut-off trend observed in the asymmetric α -alkylation of aldehydes (see Scheme 3 above). Thus, when bulky (aromatic) aldehyde substrates were used, very low conversions (<5%) were observed, with no stereocontrol. Notably, the catalyst also demonstrated excellent recoverability and reusability, maintaining both its crystallinity and catalytic activity over three cycles, conserving the same efficiency in the conversion of the starting materials into the desired product.

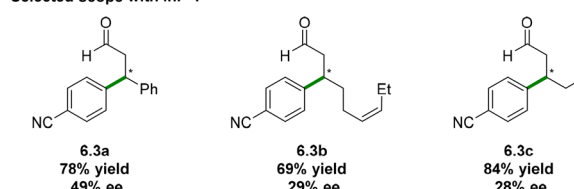
Synthetic Application



Catalyst Design



Selected scope with InP-1



Scheme 6 Chiral metal–organic frameworks (CMOFs) for the light-driven asymmetric β -functionalization of carbonyls. Adapted with permission from ref. 49. Copyright © 2017, Springer nature.

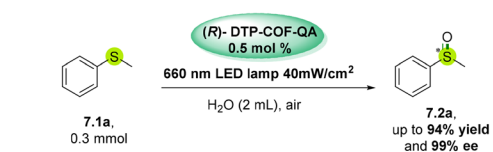
Oxidation reactions

Nitrogen-based catalytic units are not only crucial for asymmetric photoinduced alkylation/arylation reactions, but also play a pivotal role in a wide range of different transformations. A notable example has been reported by the Dong group,⁵¹ who developed a CCOF decorated with propargylamine and quaternary ammonium bromide functionalities. This material, based on a porphyrin core, efficiently catalyzed the visible light-driven enantioselective photooxidation of sulfides **7.1** to sulfoxides **7.2** in aqueous media under ambient air (Scheme 7).

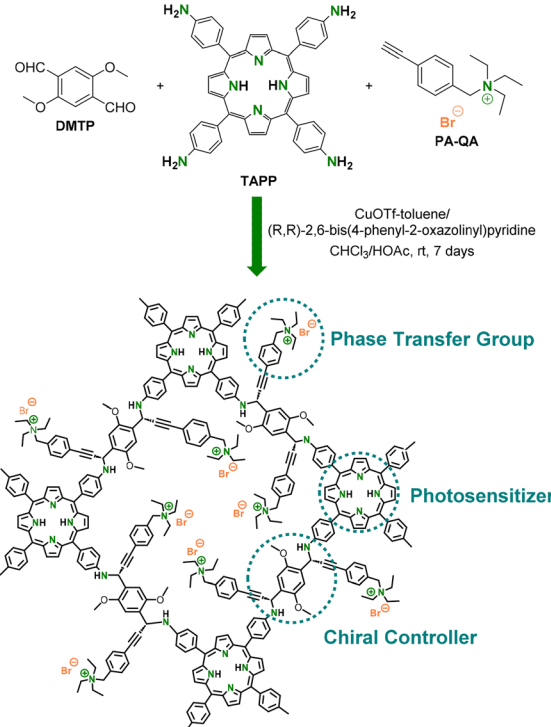
The chiral catalyst (*R*)-DTP-COF-QA, characterized by a *ca.* 1.72 nm pore size, was synthesized through a catalytic asymmetric polymerization of 2,5-dimethoxyterephthaldehyde (**DMTP**), 5,10,15,20-tetrakis(4-aminophenyl)porphyrin (**TAPP**), and a quaternary ammonium bromide-functionalized phenylacetylene derivative (**PA-QA**). Each component of the COF contributes a specific function: the porphyrin unit serves as a photosensitizer, the chiral segment formed from the **DMTP** and **PA-QA** governs stereoselectivity, and the quaternary ammonium group acts as a phase-transfer catalyst. This system



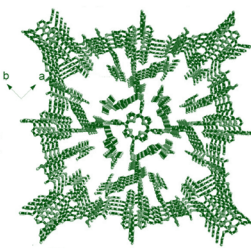
Synthetic Application



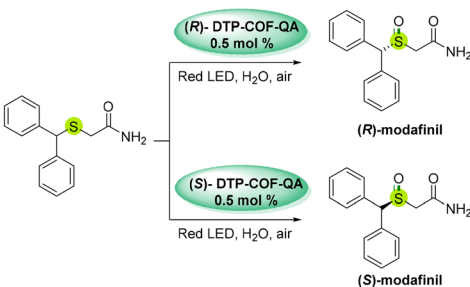
Catalyst Design



Crystal structure of (R)-DTP-COF-QA



Enantioselective preparation of modafinil



Scheme 7 Chiral covalent-organic frameworks (CCOFs) for the visible-light mediated enantioselective photooxidation of sulfides in water. Adapted with permission from ref. 51. Copyright © 2022, American Chemical Society.

demonstrated excellent performance in the model oxidation reaction of methylphenylsulfide **7.1a**, achieving up to 94% yield and 99% enantiomeric excess (ee) for the corresponding sulfone **7.2a**. Encouraged by these results, Dong's group further applied the catalyst to a more practical synthesis—the enantioselective preparation of *(R)*-modafinil, a clinically used wakefulness-promoting agent for the treatment of excessive sleepiness. Moreover, the catalyst was successfully recovered and reused over five consecutive runs, maintaining both its catalytic performance (conversion and enantiomeric excess) and crystallinity.

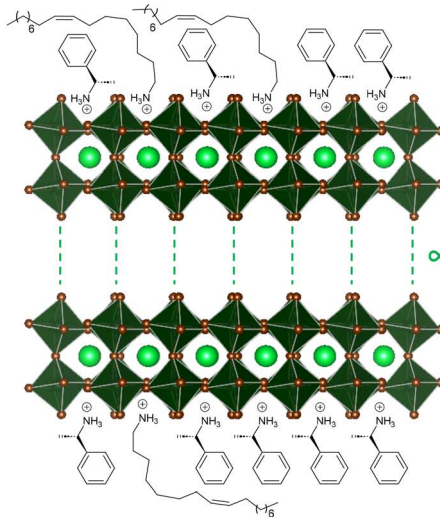
C–N bond formation

In addition to CMOFs and CCOFs, the Yan group has recently demonstrated that hybrid organic-inorganic metal-halide chiral perovskite nanocrystals (MHP-NCs)⁴² can also serve as effective heterogeneous catalysts to be applied in asymmetric photocatalysis settings.⁵² In particular, they prepared *R*- or *S*-PEA/CsPbBr₃ (**PEA**: 1-phenylethylamine) hybrid materials, which enabled the visible-light-driven asymmetric synthesis of N–C axially chiral *N*-arylidole heterocycles **8.2** from substrates **8.1**, achieving exceptional enantioselectivity of up to 99% ee and

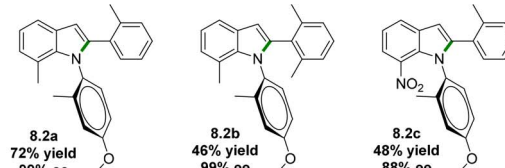
Synthetic Application



Catalyst Design



Selected scope with NC-3



Scheme 8 Photoactive chiral perovskite nanocrystals (NCs) for the asymmetric synthesis of N–C axially chiral *N*-heterocycles.



moderate to high yields (up to 72%). In this system, the surface-bound chiral **PEA** plays a crucial role in inducing atroposelectivity, whereas the free chiral **PEA** in solution has minimal influence on the stereochemical course of the process (Scheme 8). In particular, it has been proposed that, when the substrate approaches the photocatalyst surface for activation, the presence of **PEA** creates a chiral ligand-site capable of favoring the charge-transfer event, probably through weak H-bonding. The efficiency of the developed catalytic system was further demonstrated through recycling and reusability tests. The catalyst was reused over four consecutive cycles, consistently delivering good yields (71–74%) and high enantioselectivity (90–99% ee), confirming its robustness and the effectiveness of this heterogeneous enantioselective approach.

Conclusions

This perspective has summarized the recent synthetic advances in heterogeneous asymmetric photocatalysis using chiral materials. Such derivatives feature organic scaffolds to control the stereochemical course of the studied transformations, in a way similar to the catalysts adopted in asymmetric organocatalytic transformations. We highlighted the structural diversity, synthetic versatility, and photocatalytic performance of these systems, emphasizing their potential in enabling green and efficient asymmetric transformations. These materials exhibit notable advantages due to their heterogeneous nature, which results in facilitated catalyst recoverability, low catalyst loading, and the possibility to tailor the catalytic performance through structural design (*e.g.*, by proper modification of their tunable porosity). The unique role exerted by the heterogeneous nature of the catalyst, with the desired reactivity often taking place within the confined space of catalyst pores,^{46,49} has profound consequences. On one hand, a lack of reactivity is expected if the size or shape of the substrate is incompatible with the catalyst, however, such behavior may also be exploited to design selective processes toward substrates that can conveniently diffuse within catalyst pores.

While up to now a large fraction of the available reports leveraged on systems incorporating nitrogen-based chiral components, the field is rapidly expanding to harness a variety of functional groups capable of vehiculating asymmetric induction, in turn benefiting from the knowledge already available in the more mature realm of asymmetric organocatalysis. On the other hand, the remarkable tunability of the electronic structure in metal halide perovskites NCs enables the design of chiral systems for enantioselective photoreactions *via* the use of chiral capping agents. Although still in its early stage, the application of chiral perovskites is expected to expand rapidly, leveraging their well-established capability to activate a broad range of organic substrates. At the same time, the exploitation of different materials could boost the development of the field, as in the case of self-assembled supramolecular materials.⁵⁶

Looking ahead, we foresee exciting opportunities for these materials beyond organic synthesis. Their structural tunability, sustainability, and light-driven activation make them promising

candidates not only in industrial-scale enantioselective synthesis and pharmaceutical manufacturing but also in fields such as chiral sensing, enantioselective separation, and green energy conversion technologies. In particular, the development of chiral frameworks, including novel perovskite-based materials, offers a promising direction toward multifunctional systems with broader applicability.

In conclusion, our Perspective establishes a direct link between the field of heterogeneous photocatalysis and asymmetric organocatalysis, stimulating the exchange of knowledge between these two fields and fostering additional works from research groups with different expertise and background, hopefully accelerating the development of this emerging research endeavor.

Author contributions

Camilla Callegari: conceptualisation (lead), data curation (lead), writing – original and revised draft (lead), review and editing. Marco Moroni: data curation, review and editing. Davide Ravelli: conceptualisation, writing – original and revised draft, review and editing, supervision and funding acquisition. Lorenzo Malavasi: writing – original and revised draft, review and editing, supervision and funding acquisition.

Conflicts of interest

There are no conflicts to declare.

Data availability

No primary research results, software or code have been included and no new data were generated or analysed as part of this review.

Acknowledgements

This project received funding from the European Union's Horizon Europe research and innovation program under Grant Agreement 101046836 (project acronym "CATART"). The publication reflects only the author's views, and the European Union is not liable for any use that may be made of the information content therein. C. C. acknowledges financial support by the CATART project *via* a PhD grant.

Notes and references

- 1 J. R. Brandt, F. Salerno and M. J. Fuchter, *Nat. Rev. Chem.*, 2017, **1**, 0045.
- 2 P. Jeschke, *Pest Manag. Sci.*, 2025, **81**, 1697–1716.
- 3 R. U. McVicker and N. M. O'Boyle, *J. Med. Chem.*, 2024, **67**, 2305–2320.
- 4 F. Evers, A. Aharony, N. Bar-Gill, O. Entin-Wohlman, P. Hedegård, O. Hod, P. Jelinek, G. Kamieniarz, M. Lemeshko, K. Michaeli, V. Mujica, R. Naaman, Y. Paltiel, S. Refaelly-Abramson, O. Tal, J. Thijssen, M. Thoss, J. M. van Ruitenbeek, L. Venkataraman,



D. H. Waldeck, B. Yan and L. Kronik, *Adv. Mater.*, 2022, **34**, 2106629.

5 A. Garg, D. Rendina, H. Bendale, T. Akiyama and I. Ojima, *Front. Chem.*, 2024, **12**, 1398397.

6 B. M. Trost, *Proc. Natl. Acad. Sci. U. S. A.*, 2004, **101**, 5348–5355.

7 R. Noyori, *Angew. Chem., Int. Ed.*, 2002, **41**, 2008–2022.

8 The Nobel Prize in Chemistry 2021, *NobelPrize.org, Nobel Prize Outreach 2025*, <https://www.nobelprize.org/prizes/chemistry/2021/summary/>, accessed 21 July 2025.

9 O. García Mancheño and M. Waser, *Eur. J. Org. Chem.*, 2023, **26**, e202200950.

10 S.-H. Xiang and B. Tan, *Nat. Commun.*, 2020, **11**, 3786.

11 S. Bertelsen and K. A. Jørgensen, *Chem. Soc. Rev.*, 2009, **38**, 2178–2189.

12 H. Pellissier, *Tetrahedron*, 2007, **63**, 9267–9331.

13 D. Krištofíková, V. Modrocká, M. Mečiarová and R. Šebesta, *ChemSusChem*, 2020, **13**, 2828–2858.

14 T. C. Nugent, A. E. de Vos, I. Hussain, H. A. El Damrany Hussein and F. Goswami, *Eur. J. Org. Chem.*, 2022, **2022**, e202100529.

15 A. Del Vecchio, A. Sinibaldi, V. Nori, G. Giorgianni, G. Di Carmine and F. Pesciaioli, *Chem.-Eur. J.*, 2022, **28**, e202200818.

16 J. Duan and P. Li, *Catal. Sci. Technol.*, 2014, **4**, 311–320.

17 H. Jiang, L. Albrecht and K. A. Jørgensen, *Chem. Sci.*, 2013, **4**, 2287–2300.

18 M. Nielsen, D. Worgull, T. Zweifel, B. Gschwend, S. Bertelsen and K. A. Jørgensen, *Chem. Commun.*, 2011, **47**, 632–649.

19 L.-W. Xu, J. Luo and Y. Lu, *Chem. Commun.*, 2009, 1807–1821.

20 P. Melchiorre, M. Marigo, A. Carbone and G. Bartoli, *Angew. Chem., Int. Ed.*, 2008, **47**, 6138–6171.

21 B. List, *Synlett*, 2001, **2001**, 1675–1686.

22 T. Parvin, R. Yadav and L. H. Choudhury, *Org. Biomol. Chem.*, 2020, **18**, 5513–5532.

23 B. Atashkar, M. A. Zolfigol and S. Mallakpour, *Mol. Catal.*, 2018, **452**, 192–246.

24 Z. Zhang and P. R. Schreiner, *Chem. Soc. Rev.*, 2009, **38**, 1187–1198.

25 S. J. Connolly, *Chem.-Eur. J.*, 2006, **12**, 5418–5427.

26 R. Kshatriya, *ACS Omega*, 2023, **8**, 17381–17406.

27 C. Stephenson, T. Yoon and D. W. C. MacMillan, *Visible Light Photocatalysis in Organic Chemistry*, Wiley, Weinheim, 2018.

28 D. Ravelli, D. Dondi, M. Fagnoni and A. Albini, *Chem. Soc. Rev.*, 2009, **38**, 1999–2011.

29 S. Crespi and M. Fagnoni, *Chem. Rev.*, 2020, **120**, 9790–9833.

30 Y. Li, Z. Huangfu, Y. Li, X. Song, Y. Duan, Y. Zhang and X. Li, *ACS Catal.*, 2025, **15**, 7543–7577.

31 M. J. Genzink, J. B. Kidd, W. B. Swords and T. P. Yoon, *Chem. Rev.*, 2022, **122**, 1654–1716.

32 W. Yao, E. A. Bazan-Bergamino and M. Ngai, *ChemCatChem*, 2022, **14**, e202101292.

33 T. Li, Y.-T. Chen, X.-B. Zhang, R.-R. Du, L.-N. Ma and Y.-Q. Lan, *Chem. Soc. Rev.*, 2025, **54**, 5912–5960.

34 T. A. Gazis, V. Ruta and G. Vilé, *ACS Catal.*, 2025, **15**, 6852–6873.

35 X. Qiu, Y. Zhang, Y. Zhu, C. Long, L. Su, S. Liu and Z. Tang, *Adv. Mater.*, 2021, **33**, 2001731.

36 G. Szöllösi, *Catal. Sci. Technol.*, 2018, **8**, 389–422.

37 H. Zhang, S. Liu, Q. Zhang, K. Hong, J. Li, X. Yan and J. Pan, *ChemistrySelect*, 2025, **10**, e202405224.

38 Y. Zhang, Y. Zhu, W. Zhou, X. Qiu and Z. Tang, *Part. Part. Syst. Charact.*, 2018, **35**, 1700280.

39 H.-G. Jin, P.-C. Zhao, Y. Qian, J.-D. Xiao, Z.-S. Chao and H.-L. Jiang, *Chem. Soc. Rev.*, 2024, **53**, 9378–9418.

40 Q. Liu, Z. Li, J. Sun, Y. Lan, J. Hu, Y. Xiao, F. Yang and D. Gao, *J. Sep. Sci.*, 2025, **48**, e70101.

41 P. Liu, W. Dai, X. Shen, X. Shen, Y. Zhao and J.-J. Liu, *Molecules*, 2024, **29**, 5006.

42 M. Moroni, C. Coccia and L. Malavasi, *Chem. Commun.*, 2024, **60**, 9310–9327.

43 Y. Lin, J. Guo, J. San Martin, C. Han, R. Martinez and Y. Yan, *Chem.-Eur. J.*, 2020, **26**, 13118–13136.

44 Y.-W. Su, C. Pan, T.-Y. Sun and Y.-Q. Zou, *Chem. Synth.*, 2025, **5**, 10.

45 D. A. Nicewicz and D. W. C. MacMillan, *Science*, 2008, **322**, 77–80.

46 P. Wu, C. He, J. Wang, X. Peng, X. Li, Y. An and C. Duan, *J. Am. Chem. Soc.*, 2012, **134**, 14991–14999.

47 Y. Zhang, J. Guo, L. Shi, Y. Zhu, K. Hou, Y. Zheng and Z. Tang, *Sci. Adv.*, 2017, **3**, e1701162.

48 T. He, R. Liu, S. Wang, I. K. W. On, Y. Wu, Y. Xing, W. Yuan, J. Guo and Y. Zhao, *J. Am. Chem. Soc.*, 2023, **145**, 18015–18021.

49 Z. Xia, C. He, X. Wang and C. Duan, *Nat. Commun.*, 2017, **8**, 361.

50 M. T. Pirnot, D. A. Rankic, D. B. C. Martin and D. W. C. MacMillan, *Science*, 2013, **339**, 1593–1596.

51 X. Kan, J.-C. Wang, Z. Chen, J.-Q. Du, J.-L. Kan, W.-Y. Li and Y.-B. Dong, *J. Am. Chem. Soc.*, 2022, **144**, 6681–6686.

52 K. Mishra, D. Guyon, J. San Martin and Y. Yan, *J. Am. Chem. Soc.*, 2023, **145**, 17242–17252.

53 W. Gong, Z. Chen, J. Dong, Y. Liu and Y. Cui, *Chem. Rev.*, 2022, **122**, 9078–9144.

54 H.-C. Ma, Y.-N. Sun, G.-J. Chen and Y.-B. Dong, *Chem. Sci.*, 2022, **13**, 1906–1911.

55 X. Cui, Q. Ruan, X. Zhuo, X. Xia, J. Hu, R. Fu, Y. Li, J. Wang and H. Xu, *Chem. Rev.*, 2023, **123**, 6891–6952.

56 X. Tan, P. Jeyakkumar, Y. Zhang, L. Chu, Y. Hao, S. Li, K. Wang and X. Hu, *cMat*, 2024, **1**, e31.

